Desalination and Water Treatment
www.deswater.com

doi: 10.5004/dwt.2023.29329

286 (2023) 40–51
February

Mechanical analyses of hollow-fibre water treatment membranes

M. Ozdemir[a], S. Oterkus[a,*], E. Oterkus[a], I. Amin[a,b], A. El-Aassar[c], H. Shawky[c]

[a]*Department of Naval Architecture, Ocean and Marine Engineering, University of Strathclyde, Glasgow, UK, emails: selda.oterkus@strath.ac.uk (S. Oterkus), murat.ozdemir@strath.ac.uk (M. Ozdemir), erkan.oterkus@strath.ac.uk (E. Oterkus), i.amin@strath.ac.uk (I. Amin)*
[b]*Department of Naval Architecture and Marine Engineering, Port Said University, Port Said, Egypt*
[c]*Egypt Desalination Research Center of Excellence (EDRC), Desert Research Centre, Cairo, Egypt, emails: hameed_m50@yahoo.com (A. El-Aassar), shawkydrc@hotmail.com (H. Shawky)*

Received 24 July 2022; Accepted 24 January 2023

ABSTRACT

The long-term durability of water treatment membranes under working pressures is considered to be vital; however, there has not been a comprehensive analysis framework for that purpose. We therefore carry out a series of mechanical analyses for the hollow fibre water treatment systems under filtration and backwashing conditions. A series of quasi-static analyses are performed initially; and the stress conditions are determined under the operational filtration and backwashing pressures. Afterwards, the viscoelastic effects are invoked for the long-term deformation analysis of the hollow fibre membranes. Both quasi-static and viscoelastic analyses are performed by a commercial finite element package, ANSYS. The mechanical fatigue life predictions are then carried out considering the stress values from the quasi-static analyses and the long-term deformations from the viscoelastic analyses. Findings from the analyses recommend that the impact of the long-term viscous deformations on the fatigue lives are less severe compared to that of backwashing. The increase of the backwashing and filtration pressure has been found to be reducing the membrane lives significantly.

Keywords: Mechanical analysis; Hollow fibre; Membrane; Water treatment; Viscoelasticity; Fatigue; Finite element method

1. Introduction

The scarcity of the clean water has been a significant problem over the last decades. It is therefore important to utilize water resources in a more sustainable way. In this regard, re-utilization of the polluted water for different purposes, in addition to effective consumption of the existing water resources, holds a prominent place for the sustainable water management. Among the water reuse applications, membrane bioreactors play an important role [1]. The membranes for bioreactors are usually manufactured by organic and inorganic based materials. The organic based polymeric membranes are rather prevalent owing to their relatively low investment costs [2]. On the other hand, the polymeric membranes suffer from the degradation and wear caused by harsh content of the feed water, backwashing (back-pulsing) as well as the chemical cleaning [3].

The overall efficiency of the water treatment system and the permeate water quality heavily depend on the structural integrity of the membranes. On the basis of this fact, Wang et al. [4] have undertaken a comprehensive literature review work summarizing the wide range of techniques that can be employed for the mechanical response characterization. Uniaxial tensile tests are the most popular and straightforward ones among them to obtain useful data, that is, strength and stiffness of the membrane materials. The parameters, which are ideally evaluated by uniaxial tensile tests are: stress–strain relations, modulus of elasticity, yielding point, ultimate strength and elongation at break [4].

* Corresponding author.

Hou et al. [5] conducted uniaxial tests for the organic based hollow fibre membranes, and the mechanical properties of the inorganic based hollow fibre membranes were obtained by Hong and He [6]. Dynamic Mechanical Analysis (DMA) is another suitable technique to characterize the viscous behaviour of polymeric materials under various environmental conditions [7]. Viscous damping properties of the membranes can be determined by DMA under various temperature and test frequencies [8]. Emori et al. [9] performed an extensive study on the mechanical response of porous polymeric hollow fibre membranes involving both experimental and detailed finite element (FE) works. Creep deformation of the membranes was also reported by the study of Emori et al. [9].

Tng [10] performed the reliability analyses of water treatment systems in terms of membranes' mechanical failures. In that work, high cycle fatigue tests for the hollow fibre membranes were performed under simple uniaxial cyclic loads, but not the actual operational pressure conditions.

Even though the work of Tng [10] is valuable as it reports the fundamental fatigue data, the mechanical fatigue life prediction of water treatment membranes under filtration cycles has not been reported yet to the best of authors' knowledge. This issue has also been reported in the review work of Wang et al. [4].

Taking into account the lack of works on the fatigue life predictions of water treatment membranes in the open literature, we aim to present a general framework on the mechanical analysis of hollow fibre water treatment membranes under realistic operational pressure loads (under internal and external pressures). The main focus is given to fatigue life predictions; however, the viscoelastic creep deformation and its impact on the membrane performance will also be addressed in the present work. The present work currently omits the influence of chemical cleaning and membrane fouling in the fatigue life predictions due to the lack of available material data for these circumstances. However, it must be noted that the proposed framework can be effectively applied for those cases with the proper material data (S-N curve) representing the real conditions.

2. Problem setup and case studies

The hollow fibres made by polymeric materials are common for submerged type membrane bioreactors. The vacuum condition is usually generated on the permeate side in addition to hydrostatic pressure acting on the outer surface of the membrane.

In this paper, we will focus on a single fibre of a membrane module to examine its mechanical response under various loading scenarios and assumptions.

2.1. FE modelling

In the FE modelling of a fibre, we utilize the axial symmetry of the geometry and loading. One half of the membrane is modelled by ANSYS axisymmetric plane elements, Plane182, employing full integration of the stiffness matrix [11]. Invoking the full integration will ensure the stress calculation at 4 Gauss points within the quad elements. In case of stress extrapolation to the nodal points, we will be able to get more accurate stress values at the corner points of the elements, and so the more accurate fatigue life predictions.

The expanded view of the FE model is given in Fig. 1. This is the half-length model of a fibre. In this case, its length is set as 10 mm. Childress et al. [3] reported that the failure of the membranes usually occurs in the moulding and the potting resin interface. The length of the membrane will therefore be less significant. The diameters and so the wall thickness of the membrane may impact the mechanical response of the membrane. In this study, we will take single diameter case, D_{in} = 1.0 and D_{out} = 2.0 mm. The wall thickness of the membrane is 0.5 mm.

Only quad elements are employed in the modelling. The number of elements through the wall thickness is set as 5, while the length direction of the fibre is represented by 100 elements, which keeps the element aspect ratio as 1.0, which is the most ideal condition for the stress evaluation at the corner nodes of the elements.

2.1.1. Loading and boundary conditions (BCs)

Considering the resin pot on the bottom of the membrane module, the bottom section of the fibre is assumed to be clamped by constraining all displacement and rotation components on the bottom plane (Fig. 1). The top plane of the membrane is considered to be symmetry plane, which allows translation on this plane while the displacements normal to this plane is constrained. One must note that the BCs on the top plane will not have any significant effect on the mechanical life of the membrane.

In case of the filtration process, the filtration condition is enforced by uniform vacuum pressure on the permeate side. This condition can be represented accurately by uniform pressure on the external edges of the axisymmetric plane model as shown in Fig. 2a. As for the backwashing condition, the clean water with or without cleaning chemicals

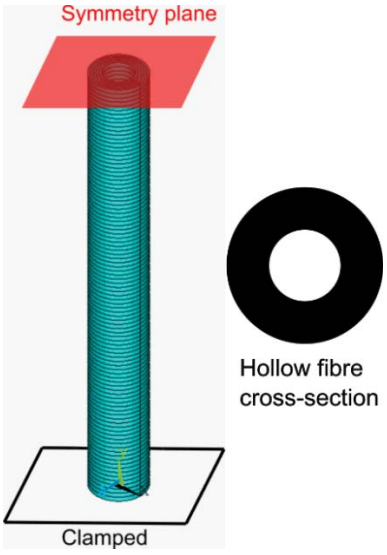

Fig. 1. Hollow fibre FE model (expanded view) and the fibre cross-section.

are pumped from the permeate side, and this condition is resembled by the uniform pressure applied on the edges of the lumen side (Fig. 2b).

The load implementation schemes are different for quasi-static and viscoelastic analyses. In case of quasi-static analyses, the load is gradually increased up to desired level (Fig. 3a). The pseudo-time expression stands for the gradual load implementation but not the real time itself [12]. This assumption is to make the numerical solution more accurate and stable by taking the large deformation effects into account. In case of viscoelastic simulations, the desired pressure level is implemented suddenly and kept constant during the simulation (Fig. 3b). The latter case allows to examine the viscous (long-term) deformations on the membranes under constant pressure level.

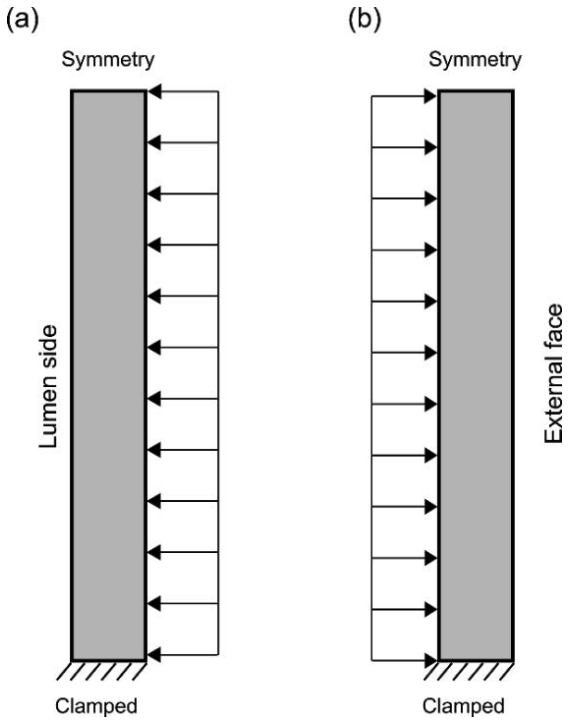

Fig. 2. Pressure implementation on the axisymmetric model: (a) filtration condition and (b) backwashing condition.

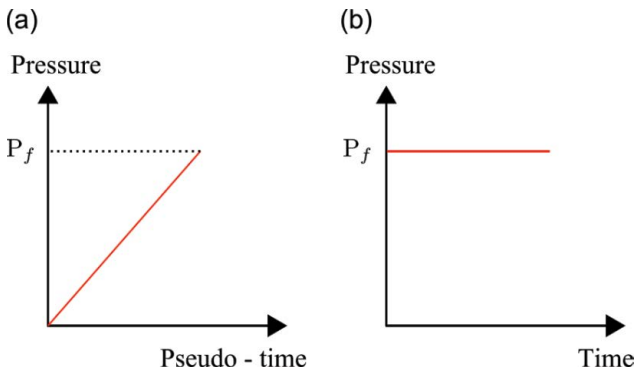

Fig. 3. Load implementation schemes for: (a) quasi-static analyses and (b) viscoelastic analyses.

2.1.2. Evaluation of the material properties

In the present work, we adopt the experimentally derived material properties from Emori et al. [9]. This adoption inherently enforces some conditions on the membrane material model. The material then becomes PVDF with the same porosity ratio with the one tested by the study of Emori et al. [9]. The reference work performs both uniaxial tensile tests and FE calculations regarding the creep behaviour of the hollow fibre membranes involving three-dimensional (3D) pore geometry. The experimental stress-strain curve for the highest strain rate, that is, $\dot{\varepsilon} = 1.4 \times 10^{-2}$ by the study of Emori et al. [9], is digitized; then the Young's modulus and yield stress are derived from the digitized curve as E = 138.9 MPa and σ_Y = 4.04 MPa. The approximate yield strain for the membrane material is derived as $\varepsilon_Y = \sigma_Y/E = 0.029$. FE quasi-static analyses are performed by employing these material properties. Although the present work adopts PVDF in the test cases, the proposed analysis framework can be employed for other polymeric membrane materials with suitable material data.

2.1.2.1. Viscoelastic properties

Since the membrane material is assumed as polymeric, we need to consider the long-term (viscous) deformation of the membrane under constant pressure loading. The long-term deformations can be represented by viscoelastic material models. In ANSYS FE code, the viscoelastic material properties are implemented by generalized Maxwell model comprised of Maxwell elements and a spring element, which are connected parallel to each other [13]. The relaxation of the viscoelastic material is mathematically represented by the Prony series, which have the exponential decay terms. The viscoelastic material properties are ideally provided by the relaxation of the shear modulus as expressed below by a Prony series expression.

$$G(t) = G_\infty + \sum_{i=1}^{N_M} G_i \times e^{(-t/\tau_i)} \tag{1}$$

where G_∞ denotes the shear modulus of the material when the time converges to infinity, which basically represents the elastic stiffness of the single spring element on the generalized Maxwell model. G_i is shear modulus of each Maxwell element, while the relaxation time of each Maxwell element is represented by τ_i. The number of Maxwell elements in the model is defined as N_M.

For the PVDF material tested by the study of Emori et al. [9], the fundamental material properties are given previously in this section. The same material was tested under constant loads to capture the creep deformation in the same work [9]. We will take the results of the creep tests presented in the reference work to obtain viscoelastic material properties. Here, one must note that the applied load at the creep tests should be below the elastic limits so that we can ensure that the membrane deformation comprises only elastic and viscous parts. In this regard, we have chosen the creep test result for 3 N axial loading by the study of Emori et al. [9]. This axial load corresponds to approximately 3.6 MPa axial stress, which is below the yielding point, and is sufficiently

large to provide valuable time dependent viscoelastic data for the possible maximum loads. Once the curve provided for 3 N in Fig. 5 by the study of Emori et al. [9] has been digitized, we can convert the data to the relaxation of Young's modulus by the well-known expression as given below.

$$E(t) = \frac{\sigma}{\varepsilon(t)} \tag{2}$$

Having the time-dependent Young's modulus readily allows to evaluate the time dependent shear modulus. A nonlinear curve fitting tool can be employed to fit a curve in the form of Prony series to the discrete data at hand. By taking two exponential terms (N_M = 2) in the Prony series, a curve is fitted to the discrete shear modulus data using the nonlinear curve fitting tool of MATLAB® [14]. The mathematical expression for the fitted curve is given as:

$$G(t) = 5.228 + 8.758 \times e^{(-t/0.906)} + 31.92 \times e^{(-t/0.103)} \tag{3}$$

The parameters in Eq. (3) should be properly introduced into an FE code for the viscoelastic materials.

2.1.2.2. Fatigue properties

The mechanical fatigue life predictions will be performed for initially perfect conditions without any defects and/or cracks. In this regard, the fatigue life predictions should be performed based on the relevant S-N data. To the best of authors' knowledge, the available material fatigue data on PVDF membrane materials are limited. Tng [10] presented some useful fatigue results for the hollow fibre membranes under cyclic tensile loading. In addition to that, Solvay [15] published a design and processing guide for PVDFs. When we digitized the S-N plot [15], we realized that the coefficient C, in the $S = C \times N^{-m}$ form of expression, is slightly higher than the yield stress of the considered material. The slope coefficient is m = 0.02. By invoking this similarity between the coefficient C and the yield strength of the material, we assume an S-N curve for the PVDF membrane material in the present work. The form of the S-N relation is taken as $S = C \times N^{-m}$. The parameter C is assumed as slightly higher than the yield strength of the material as C = 4.438, and the inverse slope coefficient is adopted as m = 0.06. The S-N curve for these parameters is given in Fig. 4.

2.1.3. Test scenarios

In the present work, we consider three different filtration pressures, which will be applied as external pressures on the axisymmetric FE models. The magnitudes of the filtration pressures are selected as, P_f = 2.0,2.5 and 3.0 bar. This pressure range is common in ultrafiltration applications [16]. The backwashing pressures are to be adopted based on the recommendation of membrane manufacturers as well as the cleaning efficiency concerns. In this work, the backwashing pressures are described by the factoring coefficients of the filtration pressures as P_b = 1.0 × P_f, 1.25 × P_f, 1.5 × P_f, 2.0 × P_f and 2.5 × P_f. Kennedy et al. [17] reported that the backwashing pressure coefficient greater than 2.5 may not be efficient in terms of cleaning; what is more, the higher values may cause damage on the membrane module. However, we pick relatively higher backwashing pressures for demonstration purposes, particularly to observe their possible impacts on the estimated fatigue lives.

The filtration durations are also varied as the case studies. In the first scenario, the filtration duration is taken as 2 h, and no backwashing is applied. In this case, it is assumed that the fouling is controlled by membrane relaxation and/or air scouring. The second case is 5 h of filtration and 5–10 min of backwashing as the air scouring may not be sufficient for the cleaning of the membrane after long filtration operation. The final scenario is the longest filtration with 10 h and 15–20 min of backwashing.

3. Quasi-static FE analyses

Quasi-static analyses are performed to obtain stress values under the assumed filtration and backwashing conditions. These stress values are first utilized to check if any plastic deformations take place on the polymeric membrane walls. Then, the maximum principal stresses are used for the mechanical fatigue life predictions.

Fig. 5 shows the stress distributions for the considered minimum and maximum filtration pressures. As it is expected, the maximum equivalent stresses take place on the lumen side at the clamped edge, which are 0.464 and 0.696 MPa for P_f = 2.0 and P_f = 3.0 bar filtration pressure cases, respectively. The maximum principal stresses also occur in the same location but in the compressive form due to the external pressure, which are 0.569 and 0.853 MPa in magnitude for P_f = 2.0 and P_f = 3.0 bar filtration pressure cases, respectively. The magnitudes of the principal stresses are evidently higher than the magnitudes of the equivalent stresses.

When the loading is applied from the lumen side (backwashing condition), it can be easily understood that the maximum principal stresses take the tensile form at the same location, that is, lumen side of the clamped edge. So, it is expected that compressive-tensile stress cycles will occur at this location, which is the situation that makes this area the most probable failure location.

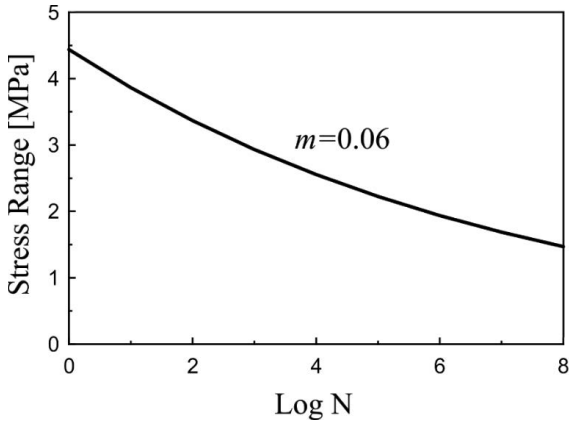

Fig. 4. S-N fatigue life curve for the considered material.

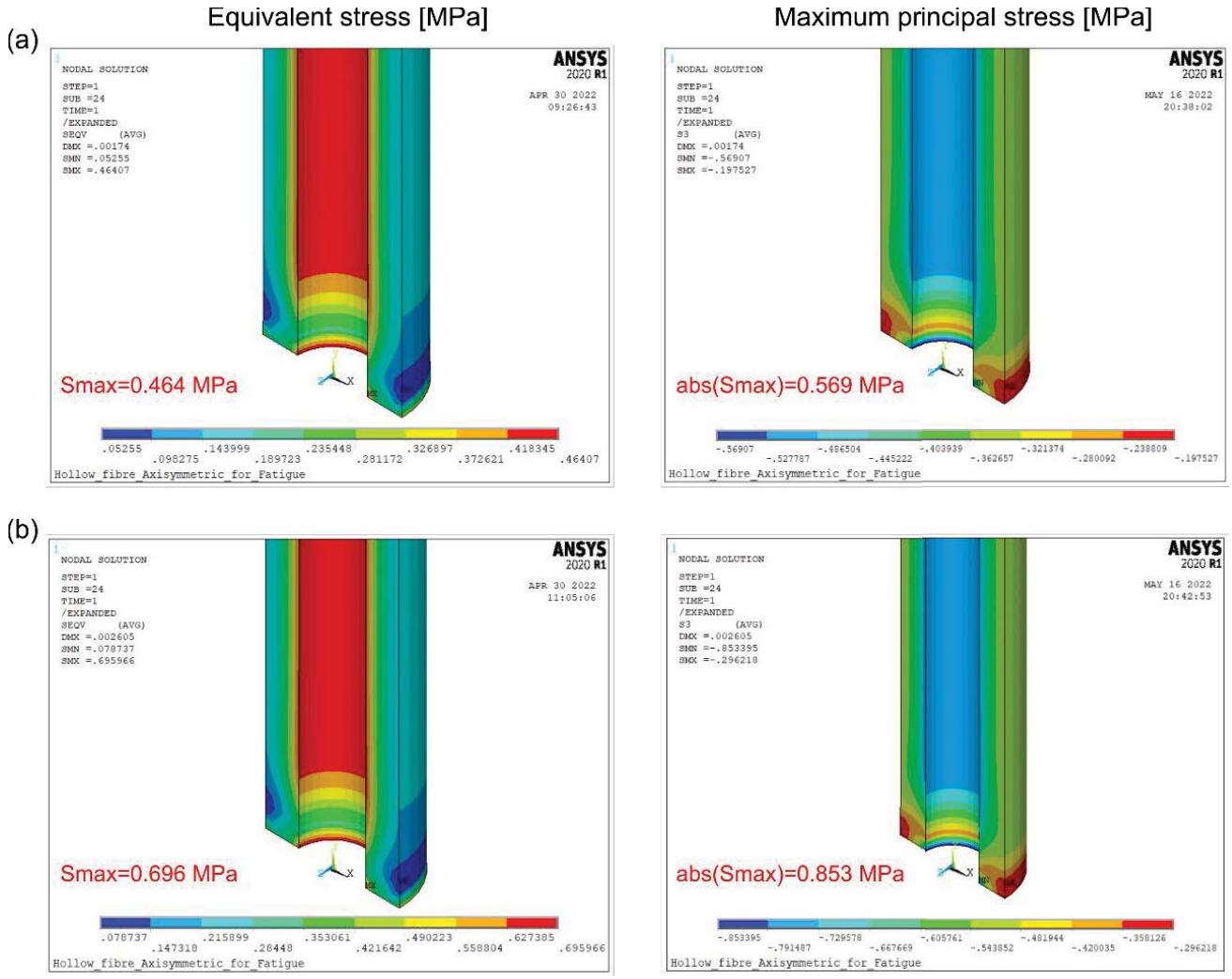

Fig. 5. Stress distributions under filtration: (a) P_f = 2.0 bar and (b) P_f = 3.0 bar.

In a similar manner, the stress distributions are provided in Fig. 6 for the backwashing condition under the maximum backwashing pressure case, that is, $P_b^{max} = 2.5 \times P_f^{max} = 7.5$ bar. In all the considered cases, the maximum values of equivalent stresses remain below the yielding point of the membrane material. The results suggest that the current configuration passes the first level control for the structural integrity assessment of the hollow fibre membranes. This condition is required but not adequate itself. A further assessment will be carried out in the following sections.

For the further assessment of the membranes, we aim to carry out fatigue life calculations using the principal stresses from this section. The maximum absolute values of the principal stresses are therefore presented in Fig. 7 for both filtration and backwashing. It must be noted that the principal stresses are compressive in Fig. 7a.

4. Viscoelastic analyses

The quasi-static analyses in the previous section should be considered as the initial check for the assessments of the membranes. Viscoelastic analyses may be considered as the elaborated assessment stage, since the long-term deformation of the polymeric materials under constant loading can be simulated by this approach.

The findings from the viscoelastic analyses may be utilized for the assessment of the permeate water quality as well as improvement of fatigue life predictions. As described in the material modelling section, the viscoelastic properties will be introduced by means of the Prony series coefficients in ANSYS FE package [13].

A viscoelastic analysis is essentially a transient dynamic analysis without inertia effects [11]. We therefore follow the procedure recommended [11]. The simulation time is equal to the filtration duration, that is, t_{sim} = 2 5 and 10 h. The time increment size is set as variable based on the convergence rate of the FE simulation. The loading scheme is defined by Fig. 3b in Section 2.1.1. Because the membrane wall is relatively thicker compared to the diameter, the numerical instabilities due to the sudden implementation of the loading can be avoided.

The viscoelastic analyses are performed only for the filtration cases since the assumed backwashing durations are significantly shorter than the considered filtration

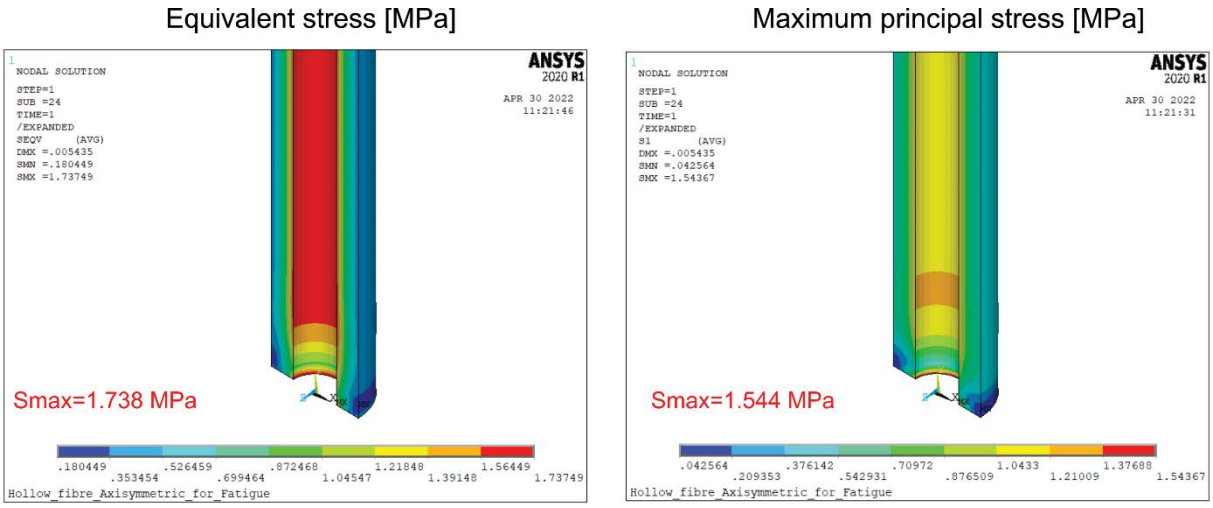

Fig. 6. Stress distributions for the backwashing condition under maximum considered pressure (P_b = 7.5 bar).

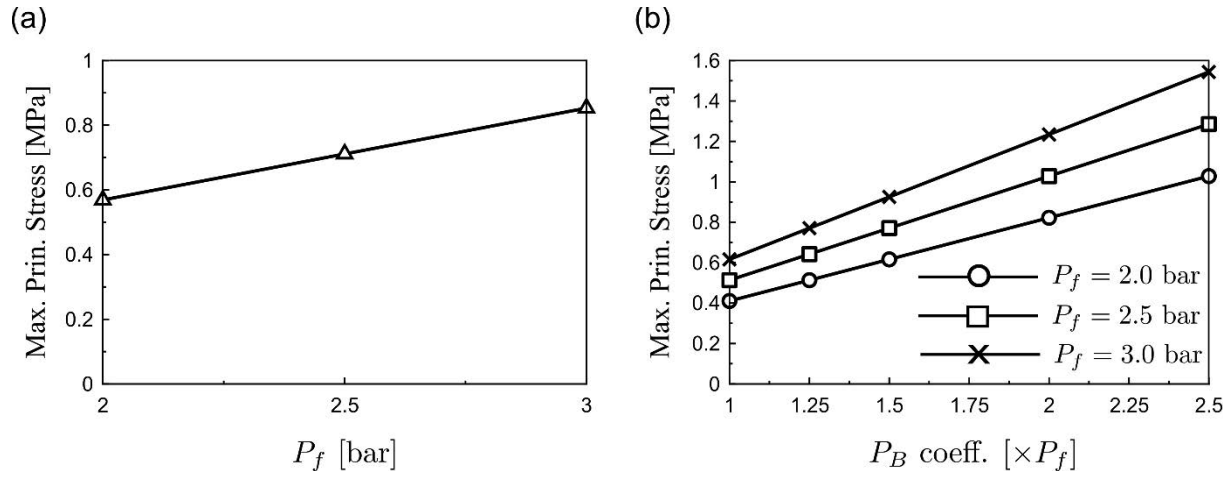

Fig. 7. Maximum absolute values of the principal stresses: (a) filtration and (b) backwashing.

durations; and the viscous deformation effects may be omitted for backwashing applications.

The stresses acting on the membrane wall remain more or less the same during the viscoelastic simulations under the same filtration pressure. We will thus focus on the displacement and strain values to assess the possible decline of the permeate water quality and the compromise of the structural integrity due to an excessive deformation.

Fig. 8 shows the increase of the maximum equivalent strain values by the time. At the beginning of the simulations (the condition that corresponds to the quasi-static analysis results), the maximum values of the equivalent strains are far below the yield strain of the material. In 10 h of filtration case, the maximum values of the strains reach and exceed the yield strain under P_f = 2.5 and 3.0 bar filtration pressures, respectively. Although these maximum values are limited to a certain location, that is, same as the maximum stress locations in Fig. 5, it is suspected that decline in the permeate water quality might occur in the water treatment system. The system would most probably remain safe for the considered filtration durations, if the filtration is P_f = 2.0 bar or lower. It must be pointed out that the exceedance of the yield strain value here does not mean the membrane experiences plastic deformation. This is an indication of the viscous deformation rather than the elastic deformation. Therefore, the membrane material is still in the elastic regime, and once the applied pressures have been removed, the membrane would recover its original shape in a sufficiently long time. The distributions of equivalent and principal stresses in Fig. 9 prove that the stress state is still in elastic region for P_f = 3.0 bar after 10 h of filtration.

Apart from the maximum equivalent strain values, the principal strains were also recorded in the viscoelastic analyses in order to include long-term deformation effects in the fatigue life calculations.

5. Mechanical fatigue life calculations

The mechanical fatigue lives of the membranes are examined under various filtration and backwashing pressures

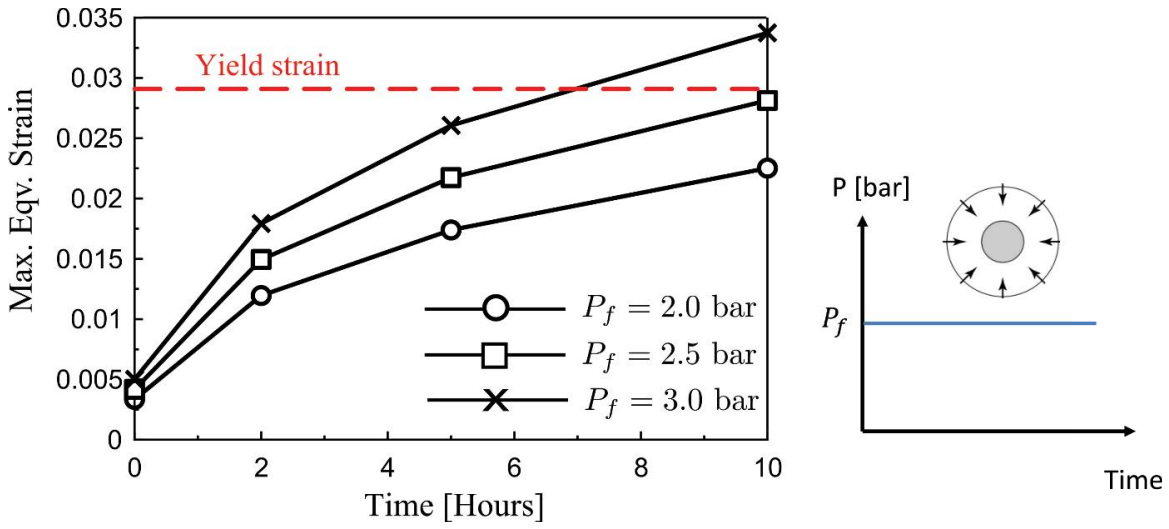

Fig. 8. Viscoelastic analysis results for different filtration pressures and durations.

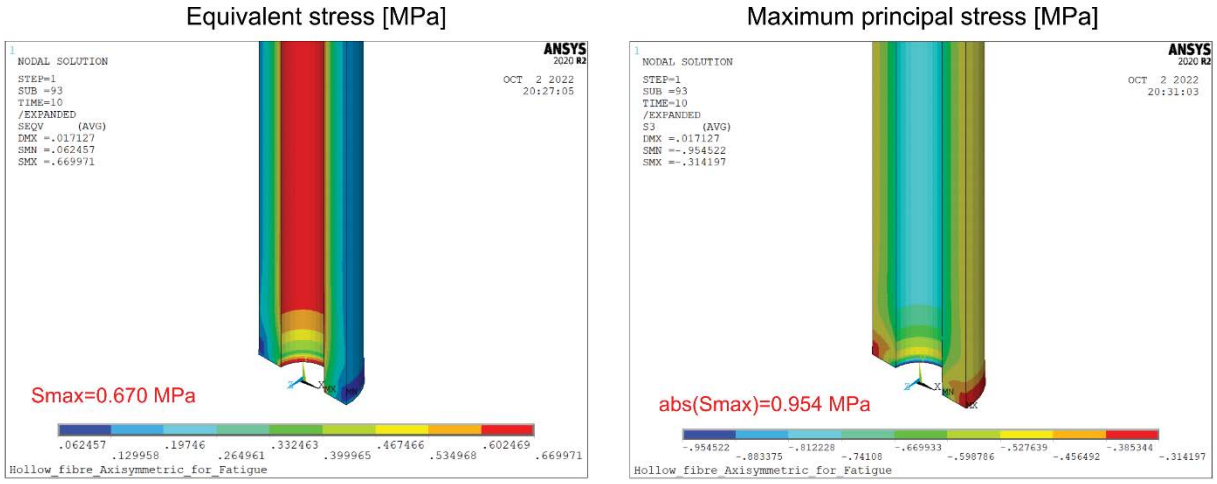

Fig. 9. Stress distributions after 10 h of viscoelastic analyses under P_f = 3.0 bar.

for the certain filtration durations, that is, t_{sim} = 2.5 and 10 h. The chemical wear and corrosion of the membrane material are currently being omitted. The influence of the long-term filtration is however taken into account for the fatigue life predictions.

The fatigue parameters for the considered membrane material are given in Section 2.1.2.2. The loading procedure and one load cycle definition for the cases with and without backwashing implementation are schematically illustrated in Figs. 10 and 11, respectively.

The filtration durations are rather longer than the duration of backwashing, which can be assumed as maximum 20 min for 10 h of filtration. Depending on the application, content of the feed water and the region of the facility, the backwashing duration may show variation, but usually becomes shorter than the present assumptions. Because of this reason, the long-term viscous deformation effects are only considered for the filtration period.

In case of shorter filtrations, the membrane fouling may be controlled by the air scouring and some cleaning chemicals to avoid the impact of backwashing. So, we will also consider without backwashing case for the shortest filtration duration, that is, 2 h.

5.1. Fatigue life calculation procedure

A simplified fatigue analysis procedure is employed for the fatigue life predictions, which takes indirectly into account the viscous deformation effects for filtration. The procedure followed in the fatigue life predictions is presented in Fig. 12.

The procedure given in Fig. 12 can be further explained as follows. The quasi-static analyses are first undertaken for filtration process. As mentioned previously, the viscoelastic analyses should be performed afterwards. Since the duration of backwashing is shorter, it is only required to carry out quasi-static analyses for the backwashing.

Maximum principal stresses and strains at each nodal points are to be collected from the quasi-static analyses. However, only principal strains at each nodal point are

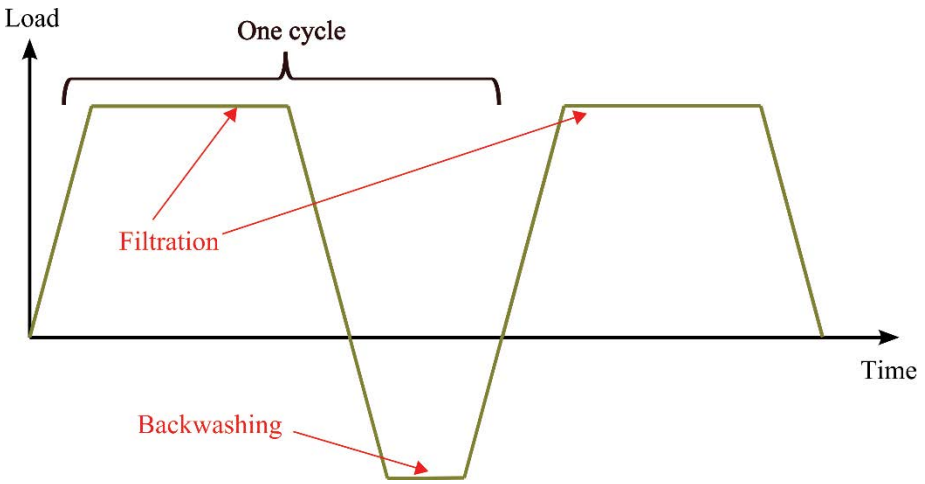

Fig. 10. Loading procedure for filtration + backwashing cycle.

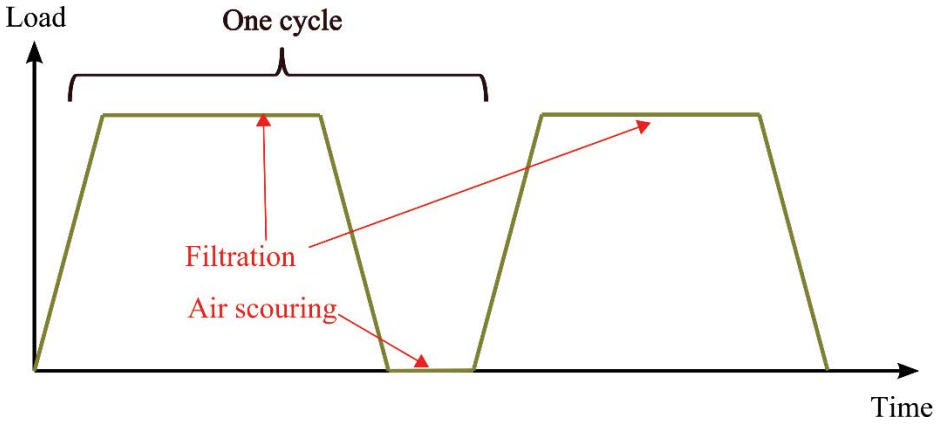

Fig. 11. Loading procedure for filtration + air scouring/membrane relaxation cycle.

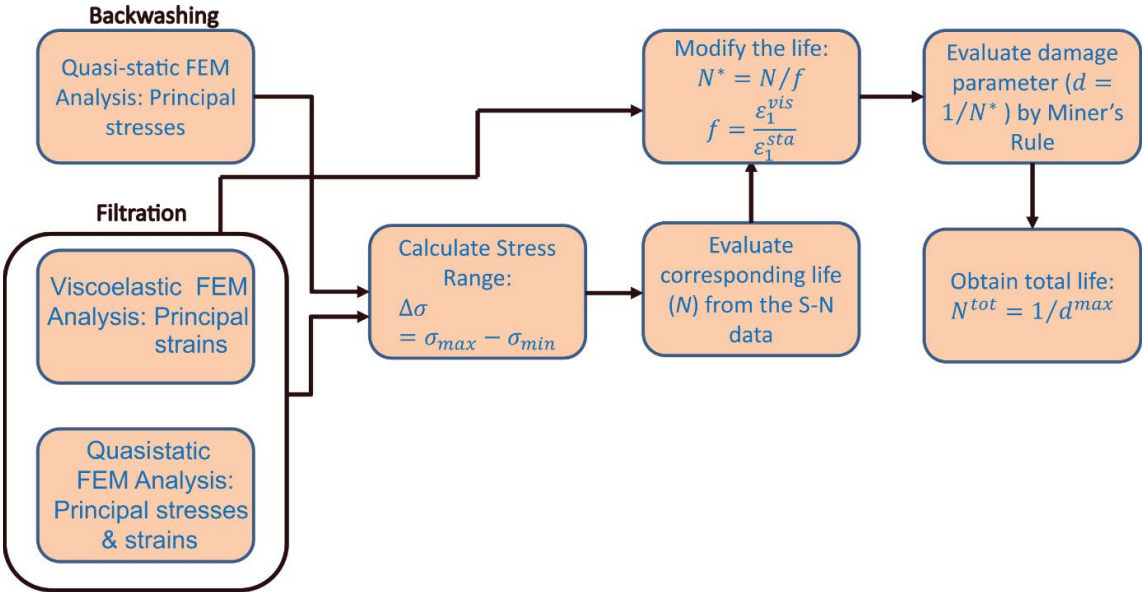

Fig. 12. Fatigue life calculation procedure for the hollow fibre membranes.

recorded from the viscoelastic simulations. The stress range will be calculated by the principal stresses from the quasi-static analyses of filtration and backwashing. Here, sign of the stress components has to be considered. Once the stress range has been calculated, the corresponding life from the S-N data is evaluated by $S = C \times N^{-m}$ expression. The calculated life then should be modified for the long-term effects. A factoring coefficient is employed for the modification purposes, which is the ratio of long-term 1st principal strain to the 1st principal strain from the quasi-static analyses for the filtration process. Afterwards, fatigue damage parameter for each cycle is obtained by the Miner's rule [18]. Finally, the total number of cycles for the fatigue life of membranes is obtained by relating it to the maximum damage parameter.

It is important to note that the frequency of loading is neglected as it is too small because of the longer filtration periods. Furthermore, the mean stress correction is not considered either, due to the lack of relevant data.

5.1.1. Miner's rule

The total fatigue damage parameter at a hotspot location is evaluated by the Miner's rule in the present study. The method is thus briefly explained here. The total damage parameter at a certain location is expressed as:

$$D = \sum_{i}^{k} d_i \tag{4}$$

where

$$d_i = \frac{n_i}{N_i} \tag{5}$$

where D represents the total damage at a certain location. The damage that occurs at each load cycle is denoted by d_i and is described in Eq. (5). The number of loading cycles at that location for a certain stress range is denoted as n, while N is the corresponding total fatigue life at the given stress range obtained by the S-N data. The total number of stress range blocks are represented by k. If the accumulated damage value, D becomes equal to 1.0 at any point on the membrane wall, it is assumed that the membrane fails due to the fatigue damage accumulation.

5.2. Fatigue life predictions

The procedure described in the previous section and the FE based stress/strain values are utilized for the membrane mechanical life predictions. The fatigue life calculations are not only performed for the designated stress hot spots, but also they are performed for all FE nodal points to capture damage distribution on the membrane wall.

Fig. 13 shows the membrane fatigue life and the fatigue damage distribution on the quarter model of the membrane for without backwashing cases. The filtration duration is 2 h, so the long-term deformation effects are less effective in total membrane life. The membrane life for the highest filtration pressure is 1.69×10^{11} cycles, which may be practically assumed as infinite. In this case, it can be said that the membrane failure would probably occur due to other factors, for example, chemical erosion or major damage due to the suspended materials in the feed water.

The damage parameter reaches the unit value (1.0) on the lumen side of the clamped edge, as expected. The damage accumulation on the inner and outer surface of the membrane wall is also visible.

The membrane lives and damage accumulation plots for the filtration durations of 5 and 10 h, respectively presented in Figs. 14 and 15. The membrane lives are given for different filtration pressures and backwashing pressure coefficients.

As similar to the without backwashing case, the membrane failure takes place on the lumen side at the clamped edge. Since the backwashing is applied as inside-out, the damage accumulation on the external surface is less significant for these cases.

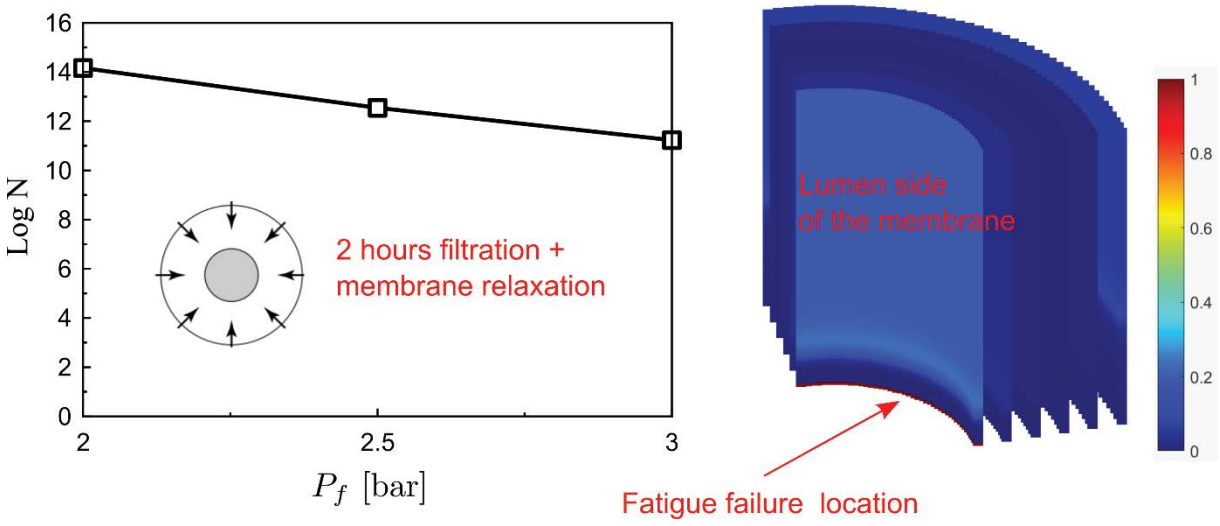

Fig. 13. Fatigue life predictions and damage accumulation for 2 h of filtration case without backwashing.

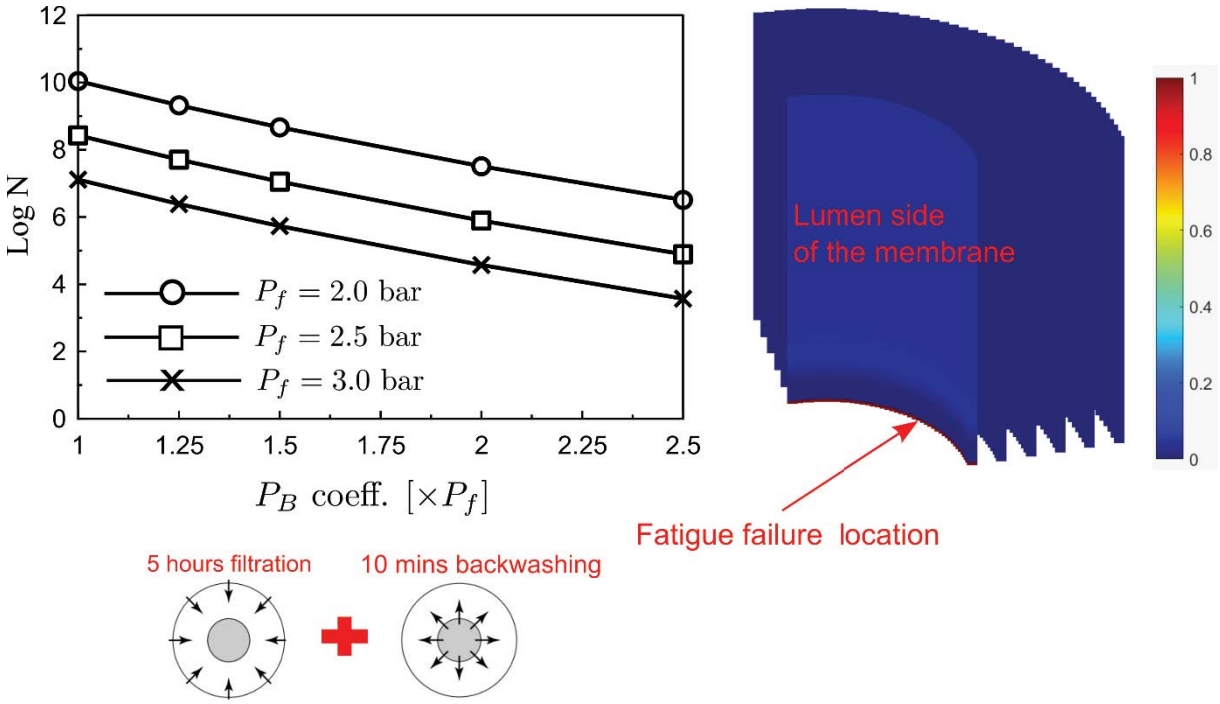

Fig. 14. Fatigue life predictions and damage accumulation for 5 h of filtration case with approximate 10 min of backwashing.

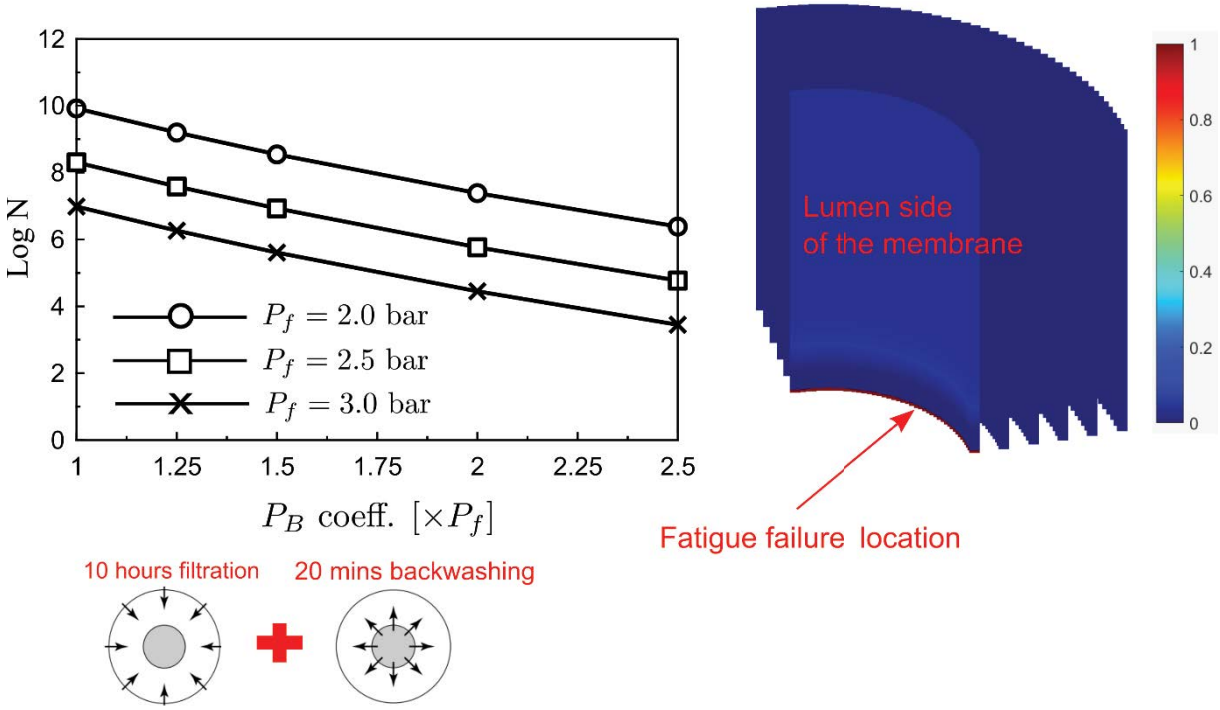

Fig. 15. Fatigue life predictions and damage accumulation for 10 h of filtration case with approximate 20 min of backwashing.

It must be noted that the predicted membrane lives are much shorter than those of the without backwashing cases. In the most severe pressure conditions, that is, P_f = 3.0 bar and P_B = 2.5 × P_f, the membrane lives are in the order of 10^3–10^4 s cycles. The membrane lives in this condition are estimated as 3,713 and 2,799 cycles for 5 and 10 h of filtration, respectively. When the backwashing pressure coefficient is increased from 1.0 to 2.5 for P_f = 3.0 bar, the membrane life reduces from 9,713,741 cycles to 2,799 cycles. These observations suggest that the influence of the long-term

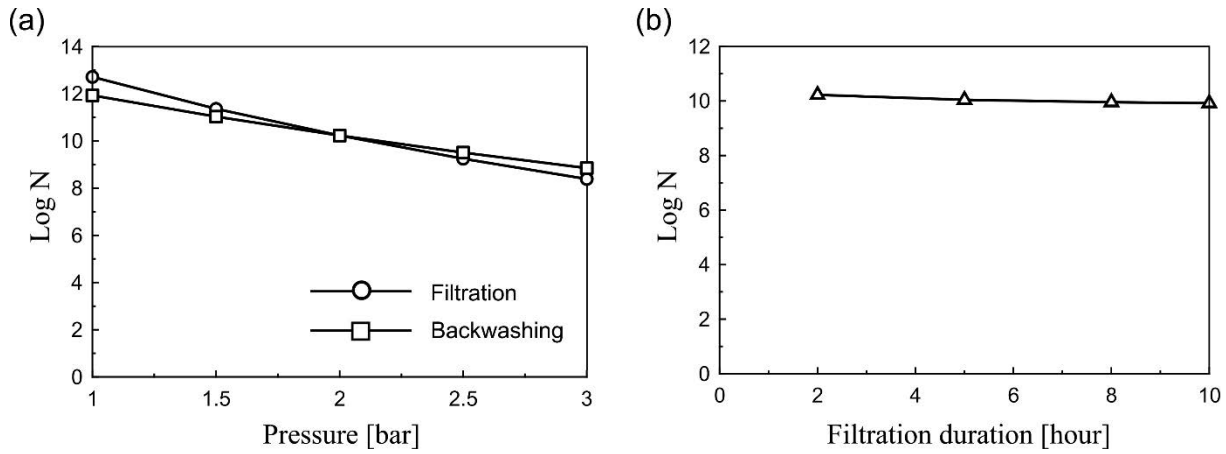

Fig. 16. Sensitivity analysis results: (a) filtration and backwashing pressures and (b) filtration duration.

deformation effects are less significant but the backwashing operation has dramatically reduced the membrane life.

5.2.1. Sensitivity analyses on the filtration parameters

In order to investigate which parameter is more influential on the predicted mechanical life of the hollow fibre membranes, we have carried out a series of sensitivity analyses. The examined parameters are filtration pressure, backwashing pressure and filtration duration.

In the sensitivity analyses of filtration pressure, we keep the backwashing pressure constant as P_b = 2.0 bar, and the filtration duration is also kept constant for all filtration pressures as 2 h. Then, the filtration pressure is varied as P_f = 1.0, 1.5, 2.0, 2.5 and 3.0 bar. A similar procedure is followed for the sensitivity analyses of backwashing pressures, that is, the filtration pressure is kept constant as P_f = 2 bar, and the filtration duration is considered as 2 h for all simulations. The sensitivity analysis results on the filtration and backwashing pressures are given in Fig. 16a.

The influence of the parameters can be examined by the slope of the log$N$ – pressure relations in Fig. 16a. It can be clearly said that the filtration pressure, which has higher negative slope, is more influential on the mechanical fatigue life of the membranes. This is mainly because of the longer filtration time as the filtration is carried out 2 h while the backwashing is around 5 min. So, viscous deformations do not take place in the backwashing operation.

The sensitivity analysis results for the filtration duration are given in Fig. 16b. It is obvious from the figure that the fatigue life – filtration duration curve is almost flat, which indicates that the effect of filtration duration on the mechanical fatigue life is less significant. It must be noted here that the filtration duration and fatigue life interaction was examined by only considering the viscous deformations, that is, higher the filtration duration, larger viscous deformations. So, this curve may be understood as the influence of viscous deformations is less significant compared to the impacts of filtration and backwashing pressures. This observation makes sense as the frequency of filtration – backwashing cycles is very low, which makes the viscous effects less significant. In high frequency loading-unloading cycles, the viscous deformations may reveal heat and degrade mechanical properties of the material.

6. Concluding remarks

In this study, the mechanical response of hollow fibre membranes under filtration and backwashing operations has been studied extensively. The structural integrity and filtration efficiency of the membranes have been examined through three stages. The first stage is quasi-static analyses. Yielding condition of the membranes has been assessed in the first stage. Moreover, the required principal stresses for the fatigue life predictions are obtained in this stage. The second stage is viscoelastic analyses, which provide the long-term deformation parameters, for example, strains that are used for the fatigue life estimations. This stage also gives some insight on the efficiency of the membrane module, as the increase of membrane deformation results in enlarged pore size. Then, the permeate water quality might be compromised due to the enlarged pore size.

The final stage is mechanical fatigue life predictions. In this stage, the viscous deformation effects from stage 2 is indirectly considered. In general, it was found that the impact of the viscous deformations on the fatigue lives are less severe compared to that of backwashing. The increase of the filtration and backwashing pressure has been found to be reducing the membrane lives significantly.

A series of sensitivity analyses have been performed in order to find out which parameter is more influential on the mechanical fatigue life of the membranes. The sensitivity analyses have revealed that the filtration pressure is the most influential parameter on the mechanical fatigue life of the membranes among the considered parameters in this study.

Acknowledgement

This work was supported by a Institutional Links grant, ID 527426826, under the Egypt-Newton-Mosharafa Fund partnership. The grant is funded by the UK Department for Business, Energy and Industrial Strategy and Science, Technology and Innovation Funding Authority (STIFA)

– project NO. 42717 (An Integrated Smart System of Ultrafiltration, Photocatalysis, Thermal Desalination for Wastewater Treatment) and delivered by the British Council.

References

[1] S. Judd, C. Judd, The MBR Book, Butterworth-Heinemann, Oxford, 2011.
[2] S.S. Madaeni, N. Ghaemi, H. Rajabi, 1 – Advances in Polymeric Membranes for Water Treatment, in Advances in Membrane Technologies for Water Treatment: Materials, Processes and Applications, Woodhead Publishing Series in Energy, Cambridge, 2015, pp 3–41.
[3] A.E. Childress, P. Le-Clech, J.L. Daugherty, C. Chen, G.L. Leslie, Mechanical analysis of hollow fiber membrane integrity in water reuse applications, Desalination, 180 (2005) 5–14.
[4] K. Wang, A.A. Abdalla, M.A. Khaleel, N. Hilal, M.K. Khraisheh, Mechanical properties of water desalination and wastewater treatment membranes, Desalination, 401 (2017) 190–205.
[5] D. Hou, J. Wang, X. Sun, Z. Ji, Z. Luan, Preparation and properties of PVDF composite hollow fiber membranes for desalination through direct contact membrane distillation, J. Membr. Sci., 405 (2012) 185–200.
[6] J. Hong, Y. He, Effects of nano sized zinc oxide on the performance of PVDF microfiltration membranes, Desalination, 302 (2012) 71–79.
[7] R.P. Chartoff, J.D. Menczel, S.H. Dillman, Dynamic Mechanical Analysis (DMA), Thermal Analysis of Polymers, John Wiley & Sons, Boca Raton, FL, USA, 2008.
[8] T.S. Chung, J.J. Qin, J. Gu, Effect of shear rate within the spinneret on morphology, separation performance and mechanical properties of ultrafiltration polyethersulfone hollow fiber membranes, Chem. Eng. Sci., 55 (2000) 1077–1091.
[9] K. Emori, T. Miura, H. Kishida, A. Yonezu, Creep deformation behavior of polymer materials with a 3D random pore structure: Experimental investigation and FEM modeling, Polym. Test., 80 (2019) 106097, doi: 10.1016/j.polymertesting.2019.106097.
[10] K.H. Tng, Mechanical Failure in Potable Reuse Plants: Component and System Reliability Considerations, Ph.D. Thesis, University of New South Wales, Sydney, 2018.
[11] ANSYS Mechanical APDL Structural Analysis Guide, ANSYS Inc., Canonsburg, PA, 2018.
[12] ANSYS Mechanical APDL Basic Analysis Guide, ANSYS Inc., Canonsburg, PA, 2018.
[13] ANSYS Mechanical APDL Material Reference, ANSYS Inc., Canonsburg, PA, 2018.
[14] MATLAB, Curve Fitting Toolbox, Mathworks, 2022. Available at: https://uk.mathworks.com/products/curvefitting.html (Accessed 25 03 2022).
[15] Solef PVDF Design & Processing Guide, Solvay.
[16] R. Singh, N.P. Hankins, Chapter 2 – Introduction to Membrane Processes for Water Treatment, N. Hankins, R. Singh, Eds., Emerging Membrane Technology for Sustainable Water Treatment, Elsevier, Amsterdam, 2016, pp 14–52.
[17] M.D. Kennedy, J. Kamanyi, S.G. Salinas Rodriguez, N.H. Lee, J.C. Schippers, G. Amy, Water Treatment by Microfiltration and Ultrafiltration, in Advanced Membrane Technology and Applications, John Wiley & Sons, New Jersey, 2008, pp 131–170.
[18] J. Schijve, Fatigue of Structures and Materials, Springer, New Jersey, USA, 2009.